remote sensing

MDPI

Technical Note

Ground-Control Networks for Image Based Surface Reconstruction: An Investigation of Optimum Survey Designs Using UAV Derived Imagery and Structure-from-Motion Photogrammetry

Toby N. Tonkin [1,2,*] and Nicholas G. Midgley [1]

[1] School of Animal, Rural and Environmental Sciences, Nottingham Trent University, Brackenhurst Campus, Southwell, Nottinghamshire NG25 0QF, UK; nicholas.midgley@ntu.ac.uk

[2] Department of Natural Sciences, University of Derby, Kedleston Road, Derby DE22 1GB, UK

* Correspondence: t.tonkin@derby.ac.uk; Tel.: +44-(0)-133-259-2673

Academic Editors: Norman Kerle, Richard Gloaguen and Prasad S. Thenkabail
Received: 5 July 2016; Accepted: 19 September 2016; Published: 21 September 2016

Abstract: The use of small UAV (Unmanned Aerial Vehicle) and Structure-from-Motion (SfM) with Multi-View Stereopsis (MVS) for acquiring survey datasets is now commonplace, however, aspects of the SfM-MVS workflow require further validation. This work aims to provide guidance for scientists seeking to adopt this aerial survey method by investigating aerial survey data quality in relation to the application of ground control points (GCPs) at a site of undulating topography (Ennerdale, Lake District, UK). Sixteen digital surface models (DSMs) were produced from a UAV survey using a varying number of GCPs (3-101). These DSMs were compared to 530 dGPS spot heights to calculate vertical error. All DSMs produced reasonable surface reconstructions (vertical root-mean-square-error (RMSE) of <0.2 m), however, an improvement in DSM quality was found where four or more GCPs (up to 101 GCPs) were applied, with errors falling to within the suggested point quality range of the survey equipment used for GCP acquisition (e.g., vertical RMSE of <0.09 m). The influence of a poor GCP distribution was also investigated by producing a DSM using an evenly distributed network of GCPs, and comparing it to a DSM produced using a clustered network of GCPs. The results accord with existing findings, where vertical error was found to increase with distance from the GCP cluster. Specifically vertical error and distance to the nearest GCP followed a strong polynomial trend (R^2 = 0.792). These findings contribute to our understanding of the sources of error when conducting a UAV-SfM survey and provide guidance on the collection of GCPs. Evidence-driven UAV-SfM survey designs are essential for practitioners seeking reproducible, high quality topographic datasets for detecting surface change.

Keywords: unmanned aerial vehicle (UAV); Structure-from-Motion (SfM); ground-control points (GCPs); digital surface model (DSM); Ennerdale

1. Introduction

The use of small Unmanned Aerial Vehicles (UAV) for acquiring aerial images is now widespread across a range of scientific disciplines (e.g., [1–6]). A surge in the use of UAVs for image acquisition has occurred simultaneously with the development of the automated photogrammetric technique commonly referred to as Structure-from-Motion (SfM) with Multi-View Stereopsis (MVS) (e.g., [7–11]). SfM-MVS allows for the rapid reconstruction of surface geometry from sufficiently overlapping imagery without the need for camera position or orientation data. A range of scientific disciplines now use an integrated approach combining the use of UAV with SfM-MVS photogrammetry (e.g., [12–15]). Validation of the SfM-MVS approach has been undertaken (e.g., [8,16–19]). Smith and Vericat [20]

and Eltner et al. [21] provide a synthesis of recent validation studies. Smith et al. [22] highlight that a fundamental weakness of the SfM-MVS approach is related to the inability to determine the quality of a given survey at the time of data acquisition.

Studies documenting optimum survey designs for practitioners integrating UAV image acquisition and SfM-MVS image processing are important if sources of error are to be minimised when acquiring datasets. An increasing number of studies have already assessed variation in the number of ground control points (GCPs) used [23], change of camera lens and associated focal length [18], flight altitude [20], use of high dynamic range (HDR) images [24], and inclusion or absence of oblique imagery [22]. The research reported here adds to our understanding of reproducibility based upon GCP number and distribution—an aspect of the UAV-SfM workflow that would benefit from further validation. Specifically, our work differs to that of Clapuyt et al. [18], because it covers a site of moderate hummocky relief with a range of aspects, rather than the 'gentle topography' assessed by Clapuyt et al. and uses a fixed focal length lens for image acquisition. Smith and Vericat [20] identify a relationship between RMSE and survey range, but highlight that further systematic validation is needed for a range of survey parameters including the distribution of GCPs and terrain type. In this study, we address aspects of GCP distribution, which is of interest due to the time intensive nature of GCP collection. Specifically, the following questions were investigated: (1) approximately how many GCPs are required for DSMs produced using UAV-SfM to provide a robust representation of surface topography and (2) how does GCP distribution affect the quality of the surface reconstruction? Answers to these questions are important for application-focused scientists seeking to conduct reliable and reproducible UAV-SfM surveys for geoscientific investigations.

2. Field Site

UAV image acquisition was conducted over an area (around 0.145 km^2) of irregular topography (former glacial "hummocky moraine") located at the head of the Ennerdale valley (54°29'N; 3°14'W) in the English Lake District, UK (Figure 1). The "hummocky moraine" located in the valley has previously been mapped and is inferred to indicate the past activity of a former Younger Dryas (12.7–11.5 ka BP) glacier within the valley [25–27]. The study area occupies an altitudinal range of ~280–330 m above sea level. The study area is currently subject to managed livestock grazing as part of an on-going re-wilding conservation programme and is free from bracken (*Pteridium* spp.) encroachment. The survey area is characterised by a complete cover of grassy vegetation, with a low and consistent sward height.

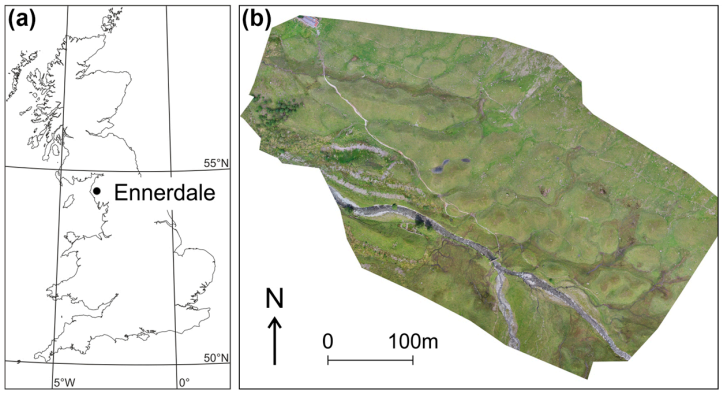

Figure 1. (**a**) The location of Ennerdale in the UK. (**b**) An orthomosiac image of the study site.

3. Materials and Methods

3.1. Data Acquisition

Images were acquired with a DJI S800 hexacopter using 11 Ah and 10 Ah, 22.2 V, 6 cell lithium polymer batteries at a pre-programmed altitude of 100 m above ground level (AGL) giving a ground

sampling distance (GSD) of ~2 cm. Flight level was determined from the Google Earth topography layer, which very coarsely allows for flight level to be maintained above the ground surface. A programmed horizontal ground speed of 2.5 $m \cdot s^{-1}$ was used and images were captured at 2-second intervals close to, or at, nadir (directly below the observation point, so a view straight down). Parallel flight lines were set up with a sidelap of 70% and an approximate forward overlap of 95%. A Canon EOS-M 18 megapixel digital camera with a 22-mm lens was used for image acquisition with Magic Lantern third-party camera firmware installed that added an intervalometer function. The approximate footprint of each image was 104 by 69 m and a total of 386 images were used. The camera was set to shutter-priority mode and a 1/1000 s shutter speed was used. Similar illumination conditions existed for each survey, although light conditions will have varied both during and between surveys. The camera was attached to a 2-axis gimbal to compensate for the in-flight movement of pitch and roll. Flights were undertaken in strong wind conditions, which at 100 m AGL are likely to have gusted to in excess of 7.5 $m \cdot s^{-1}$. The strong wind conditions meant that the UAV horizontal ground speed varied, depending on the direction of flight, above and below the programmed 2.5 $m \cdot s^{-1}$ speed. This means that forward overlap will have varied through each flight line. A total of 101 GCPs were placed within the study area (Figure 2) and surveyed with a Leica 1200 dGPS with a base station set up in the survey area. GCPs consisted of A3-sized fluorescent paper markers that were fixed to the ground. The GCP distribution was obtained by systematically placing markers on ridge crests, troughs between ridges and mid-slope positions, as this replicates likely survey design used elsewhere, rather than adopting a random or fixed-grid approach. An additional 530 spot heights were acquired with the dGPS to validate vertical error on the SfM DSMs. The positional quality (XYZ) for all dGPS points as reported in Leica Geo Office was <0.09 m, with an average point quality of 0.02 m. All data is projected using the OSGB1936 coordinate system and datum. Images were processed in Agisoft Photoscan (v. 1.1.5). Image alignment used the high accuracy setting, and a "medium" point density was used to reduce computer processing time, but still produced a high point density in each case. The 100 m AGL flights processed with the medium point density setting produced point densities of 160 points per m^2. Automatic camera optimization was used, and aggressive depth filtering was conducted to remove outlying points that were likely to represent error. Mesh production was required prior to producing a DSM on the software version that was used for the study, although this has now been revised on newer software versions. GCPs had to be manually identified as automatic recognition of GCPs does not work due to the size of GCP and survey range used here. The default marker accuracy setting of 0.005 m was used for processing. For consistency, and to facilitate comparison between DSMs, the same processing settings were used for all the DSMs produced.

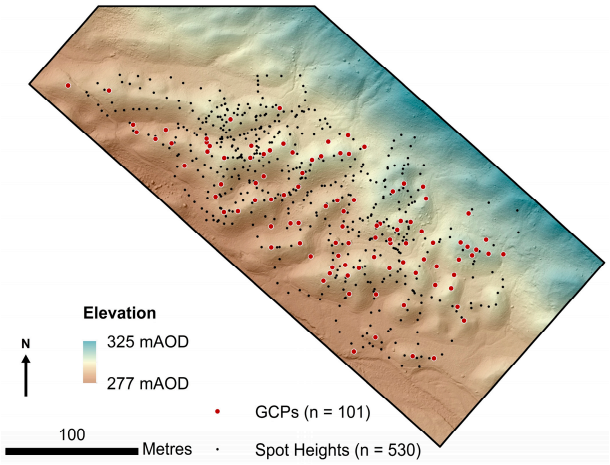

Figure 2. A digital surface model (DSM) of the Ennerdale moraines with the positions of ground control points (GCPs) (101 GCPs) and spot heights indicated (530 spot heights). The trimmed survey area displayed here is 0.071 km^2.

3.2. Data Analysis

To investigate the optimum GCP quantity for a given survey, 16 DSMs were produced using between 3 and 101 GCPs to georeference and scale each model. DSMs were exported from Agisoft Photoscan for assessment. A total of 530 dGPS spot heights were used to calculate vertical error to assess the impact that the quantity of GCPs applied had on DSM quality. The spot heights used for vertical error assessment were also collected using the Leica 1200 dGPS following the acquisition of GCPs. The 'Point Sampling Tool' in QGIS 2.8.1 was used to sample the raster surface for comparison with the dGPS height readings. Root-mean-square-error (RMSE) and mean-absolute error (MAE) were calculated as a measure of DSM quality in comparison to the dGPS spot heights. For the GCP distribution test, the sub-optimal distribution was clustered on one side of the survey area, whereas the optimal distribution was more evenly distributed throughout the survey area. The GCP distribution test used raster differencing (cell size 0.08 m) and was conducted using ArcGIS 10.3.1.

4. Results

Where 4 or more GCPs were used for DSM production, the vertical RMSE ranged between 0.059 and 0.076 m (Table 1) falling within the positional quality of the dGPS GCPs at <0.09 m. The use of 3 GCPs increased vertical error into the decimetre range with a vertical RMSE value of 0.156 m, exceeding the position quality of the dGPS ground control and spot heights (Table 1). The distribution of the GCPs used for model reconstructions are displayed in Figure 3.

When a DSM produced with a uniform distribution of GCPs (28 GCPs) was subtracted from a DSM produced using a clustered, suboptimal GCP distribution (10 GCPs), residuals were found to increase into the decimetre range (Figure 4a), exceeding 0.15 m in the extremities of the DSM. Between the two surfaces, only 60% and 42% of cells were within the $\pm$0.1 m and $\pm$0.05 range respectively, with minimum and maximum vertical differences of $-$0.091 m and 0.508 m reported. In areas of good GCP coverage the residuals typically fell within the sub-decimetre range, however, error appeared to exceed a decimetre with distance from the nearest GCP. Therefore, sampled residuals (a total of 10,000 values from across the entire area) from the differenced DSM were plotted against distance from the nearest GCP (Figure 4b) and subject to polynomial regression. A highly significant relationship between distance from the nearest GCP and the vertical residual from the DSM differencing was found (R^2 = 0.792; $P < 0.001$) (Figure 4b).

Table 1. Digital surface model (DSM) quality in relation to the random placement of ground control points (GCPs). Vertical error is measured from 530 dGPS check points using 3 GCPs resulted in a reduction of DSM quality increasing root-mean-square-error (RMSE) into the decimetre range.

Number of GCPs Used	Vertical RMSE (m)	Vertical MAE (m)	Vertical Difference (min; m)	Vertical Difference (max; m)
3	0.156	0.126	−0.462	0.427
4	0.064	0.049	−0.206	0.291
5	0.060	0.046	−0.197	0.308
7	0.062	0.048	−0.175	0.353
8	0.073	0.058	−0.192	0.257
9	0.063	0.049	−0.173	0.283
10	0.075	0.059	−0.195	0.400
15	0.076	0.061	−0.179	0.270
20	0.073	0.057	−0.190	0.280
25	0.073	0.057	−0.178	0.352
30	0.067	0.052	−0.177	0.269
40	0.066	0.050	−0.191	0.304
50	0.060	0.046	−0.143	0.282
60	0.064	0.047	−0.160	0.548
80	0.061	0.047	−0.156	0.242
101	0.059	0.045	−0.147	0.277

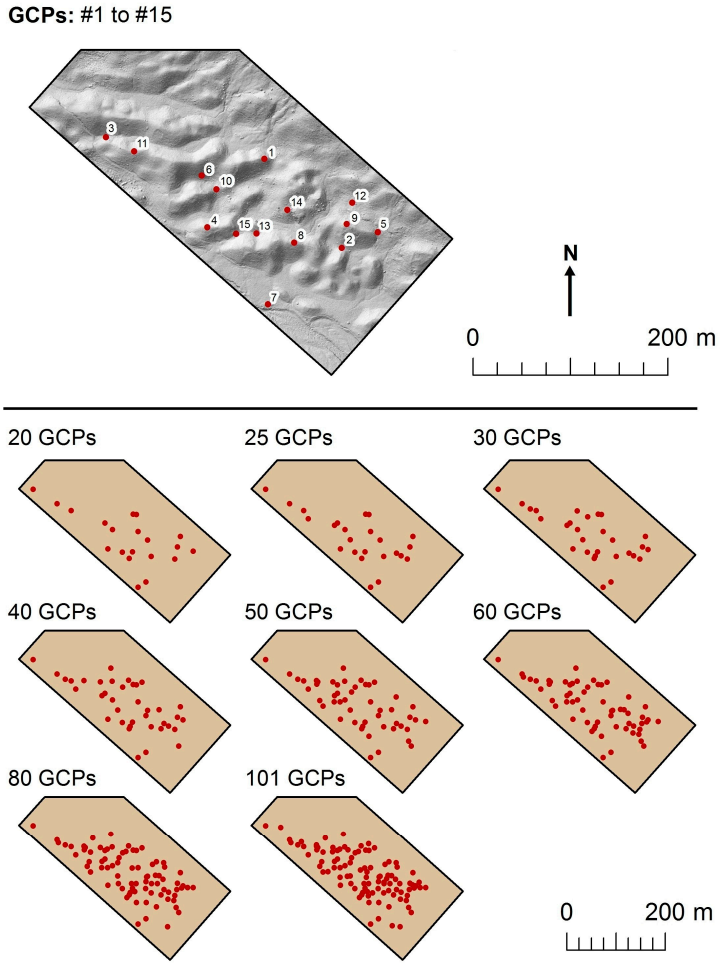

Figure 3. Ground control point (GCP) locations used to produce the 16 digital surface models (DSMs) reported in Table 1. The top panel relates to the models that use fewer than 15 GCPs. For example, for a model using 3 GCPs, the GCPs numbered 1, 2 and 3 were applied to the model. For a model using 7 GCPs, the GCPs numbered 1, 2, 3, 4, 5, 6, and 7 were applied to the model.

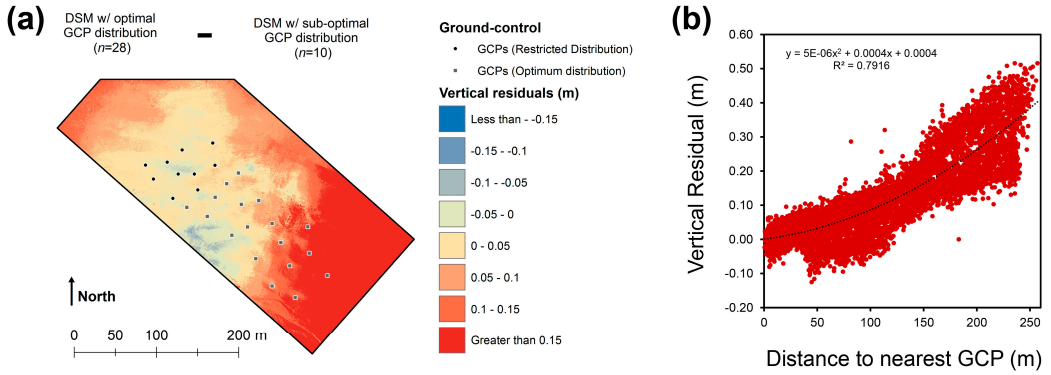

Figure 4. (**a**) The residuals assessed by subtracting a digital surface model (DSM) produced using a uniform distribution of ground control points (GCPs) from a DSM produced using a sub-optimum clustered GCP distribution. Error increases into the decimetre range with distance from the GCP cluster. (**b**) Polynomial regression of sampled cells (a total of 10,000 values) from the DSM of difference highlighting the influence of GCP distribution on error.

5. Discussion

The potential to produce a high quality survey with excellent reproducibility is a key requirement for studies using topographic data to assess change within a given environment (e.g., [3,6,12,13,28]), thus error from the georeferencing stage of the SfM-MVS workflow requires consideration. Primarily, if the GCPs are surveyed with a high error, it will undermine UAV-SfM survey reproducibility. However, all survey techniques used to generate coordinates for GCPs will contain error that will propagate in to the derived datasets. In addition to error at the point of acquisition, the distribution and quantity of GCPs appears to also strongly influence the quality of the surface reconstruction. James and Robson [11] highlight that GCPs should be located toward the edge or outside the area of interest, and whilst highlighting that 3 GCPs can be used, the collection of more GCPs is preferential for facilitating accurate reconstruction. Our study supports this assertion, with the use of 3 GCPs for a 100 m AGL UAV-SfM survey increasing the vertical RSME into the decimetre range (0.16 m). In contrast, where 4 or more GCPs were applied (up to 101), error fell to within an acceptable range that was within the suggested accuracy of the dGPS equipment used for point acquisition (Figure 4). Conventionally, for SfM-MVS, DSM quality is thought to improve as the number of GCPs applied is increased [18,21]. However, curiously, a sudden but slight increase in DSM vertical error when additional GCPs (e.g., 8–40 GCPs) were registered was documented, and a surprisingly low vertical error was achieved when just 4 GCPs were used to produce a DSM. An existing case study presented in Carrivick et al. [29] documents a reduction in error when 'suspicious' GCPs (i.e., where the positional quality is poor) were excluded prior to surface reconstruction. Similarly, the results presented here may reflect the propagation of error onto derivative data products resulting from GCPs with a poorer positional quality. One implication of this is that additional GCP collection may not necessarily improve survey quality, especially if the positional accuracy of the survey equipment is variable.

Here, the use of both 3 GCPs and 4 GCPs (or greater) may result in acceptable levels of error depending on the survey purpose, however, as previously highlighted excess GCPs did not appear to substantially improve survey quality. Based on this diminishing return, it may be tempting to reduce the quantity of GCPs collected, however, GCPs are important for assessing survey quality, which is required if multi-temporal surveys are undertaken as GCPs can also be used as validation points. Thus, the collection of excess/redundant GCPs is highly desirable if error, which will vary spatially on resulting derivative datasets, is to be better understood.

An increase in error in areas not constrained by GCPs has been documented [21]. The spatial pattern of the errors is often referred to as "doming" (e.g., [30]). This should be considered when planning a UAV-SfM survey. Traditional photogrammetry utilises nadir imagery and this is also typically used in UAV-SfM surveys. The traditional parallel flight line survey can, however, lead to doming effects on processed imagery and associated DSM when used in conjunction with low numbers of GCPs, or suboptimal GCP placement [30]. James and Robson [30] suggest the use of nadir imagery complimented with additional oblique imagery as a method to reduce the doming effect. Building on existing studies, this study quantifies the spatial component of errors from this source. The findings of this assessment accord with existing literature which highlight that a uniform coverage of GCPs is preferential across the area of interest for SfM-MVS surveys [21], and that error should be anticipated in areas not subject to ground control [21]. Critically, for the survey described here, errors from this source can enter the decimetre range in locations greater than ~100 m from the nearest GCP. It is suggested that by quantifying the magnitude of error from this source using a given survey setup and processing workflow (as documented here), a known degree of vertical error can be anticipated on surveys, which may be beneficial where multi-temporal surveys are used to quantify surface change.

6. Conclusions

Here, the GCP requirements of the SfM-MVS workflow are investigated, providing a case study that can be used to inform the implementation of future UAV surveys. Specifically, diminishing returns were found when GCPs were randomly included for model generation, with the use of $\geq$4 GCPs

for each model resulting in vertical errors within the suggested position point quality range of the dGPS equipment used to survey the GCPs. The use of 3 GCPs resulted in DSM vertical errors entering the decimetre range (0.16 m). Vertical errors exceeding a decimetre were found at distances greater than ~100 m from the nearest GCP when a suboptimal distribution of GCPs was applied to a model. Critically, this research demonstrates the importance of a uniform GCP spatial distribution where highly accurate data are required. This study also highlights that a balance can be struck between GCP quantity and survey quality, which is important to consider due to the time-intensive nature of GCP collection.

Acknowledgments: Rachel Oakley, the Project Officer for Wild Ennerdale, coordinated approval to undertake the research at Ennerdale and Michael Hine, Administrative Officer at the Forestry Commission, gave permission to use the forestry access track to the site. Nottingham Trent University provided funding for travel, accommodation and equipment. The insightful comments provided by four reviewers helped improve the focus of the manuscript.

Author Contributions: T.N.T. and N.G.M. contributed equally to this study.

Conflicts of Interest: The authors declare no conflict of interest.

References

1. Anderson, K.; Gaston, K.J. Lightweight unmanned aerial vehicles will revolutionize spatial ecology. *Front. Ecol. Environ.* **2013**, *11*, 138–146. [CrossRef]
2. Bemis, S.P.; Micklewaite, S.; Turner, D.; James, M.R.; Akciz, S.; Thiele, S.T.; Bangash, H.A. Ground-based and UAV-based photogrammetry: A multi-scale, high-resolution mapping tool for structural geology and paleoseismology. *J. Struct. Geol.* **2014**, *69*, 163–178. [CrossRef]
3. Lucieer, A.; de Long, S.M.; Turner, D. Mapping landslide displacements using Structure from Motion (SfM) and image correlation of multi-temporal UAV photography. *Prog. Phys. Geogr.* **2014**, *38*, 97–116. [CrossRef]
4. Lucieer, A.; Turner, D.; King, D.H.; Robinson, S.A. Using an Unmanned Aerial Vehicle (UAV) to capture micro-topography of Antarctic moss beds. *Int. J. Appl. Earth Obs. Geoinf.* **2014**, *27*, 53–62. [CrossRef]
5. Woodget, A.; Carbonneau, P.; Visser, F.; Maddock, I. Quantifying submerged fluvial topography using hyperspatial resolution UAS imagery and structure from motion photogrammetry. *Earth Surf. Proc. Landf.* **2014**, *40*, 47–64. [CrossRef]
6. Bhardwaj, A.; Sam, L.; Akanksha; Martín-Torresa, F.J.; Kumar, R. UAVs as remote sensing platform in glaciology: Present applications and future prospects. *Remote Sens. Environ.* **2016**, *175*, 196–204. [CrossRef]
7. Verhoeven, G. Taking computer vision aloft—Archaeological three-dimensional reconstructions from aerial photographs with Photoscan. *Archaeol. Prospect.* **2011**, *18*, 67–73. [CrossRef]
8. Westoby, M.J.; Brasington, J.; Glasser, N.F.; Hambrey, M.J.; Reynolds, J.M. 'Structure-from-Motion' photogrammetry: A low-cost, effective tool for geoscience applications. *Geomorphology* **2012**, *179*, 300–314. [CrossRef]
9. Javernick, L.; Brasington, J.; Caruso, B. Modeling the topography of shallow braided rivers using Structure-from-Motion photogrammetry. *Geomorphology* **2014**, *213*, 166–182. [CrossRef]
10. Nolan, M.; Larsen, C.; Sturm, M. Mapping snow depth from manned aircraft on landscape scales at centimeter resolution using structure-from-motion photogrammetry. *Cryosphere* **2015**, *9*, 1445–1463. [CrossRef]
11. James, M.R.; Robson, S. Straightforward reconstruction of 3D surfaces and topography with a camera: Accuracy and geoscience application. *J. Geophys. Res. Earth Surf.* **2012**, *117*. [CrossRef]
12. Eltner, A.; Braumgart, P.; Maas, H.-G.; Faust, D. Multi-temporal UAV data for automatic measurement of rill and interrill erosion on loess soil. *Earth Surf. Process. Landf.* **2014**, *40*, 741–755. [CrossRef]
13. Tonkin, T.N.; Midgley, N.G.; Cook, S.J.; Graham, D.J. Ice-cored moraine degradation mapped and quantified using an unmanned aerial vehicle: A case study from a polythermal glacier in Svalbard. *Geomorphology* **2016**, *258*, 1–10. [CrossRef]
14. Ryan, J.C.; Hubbard, A.L.; Box, J.E.; Todd, J.; Christoffersen, P.; Carr, J.R.; Holt, T.O.; Snooke, N. UAV photogrammetry and structure from motion to assess calving dynamics at Store Glacier, a large outlet draining the Greenland ice sheet. *Cryosphere* **2015**, *9*, 1–11. [CrossRef]
15. Long, N.; Millescamps, B.; Guillot, B.; Pouget, F.; Bertin, X. Monitoring the topography of a dynamic tidal inlet using UAV imagery. *Remote Sens.* **2016**, *8*, 387. [CrossRef]

16. Fonstad, M.A.; Dietrich, J.T.; Courville, B.C.; Jensen, J.L.; Carbonneau, P.E. Topographic structure from motion: A new development in photogrammetric measurement. *Earth Surf. Process. Landf.* **2013**, *38*, 421–430. [CrossRef]
17. Tonkin, T.N.; Midgley, N.G.; Graham, D.J.; Labadz, J.C. The potential of small unmanned aircraft systems and structure-from-motion for topographic surveys: A test of emerging integrated approaches at Cwm Idwal, North Wales. *Geomorphology* **2014**, *226*, 35–43. [CrossRef]
18. Clapuyt, F.; Veerle, V.; Van Oost, K. Reproducibility of UAV-based earth topography reconstructions based on Structure-from-Motion algorithms. *Geomorphology* **2016**, *260*, 4–15. [CrossRef]
19. Jaud, M.; Passot, S.; Le Bivic, R.; Delacourt, C.; Grandjean, P.; Le Dantec, N. Assessing the accuracy of high resolution digital surface models computed by PhotoScan® and MicMac® in sub-optimal survey conditions. *Remote Sens.* **2016**, *8*, 465. [CrossRef]
20. Smith, M.W.; Vericat, D. From experimental plots to experimental landscapes: Topography, erosion and deposition in sub-humid badlands from Structure-from-Motion photogrammetry. *Earth Surf. Process. Landf.* **2015**, *40*, 1656–1671. [CrossRef]
21. Eltner, A.; Kaiser, A.; Castillo, C.; Rock, G.; Neugirg, F.; Abellán, A. Image-based surface reconstruction in geomorphometry–merits, limits and developments. *Earth Surf. Dyn.* **2016**, *4*, 359–389. [CrossRef]
22. Smith, M.W.; Carrivick, J.L.; Quincey, D.J. Structure from motion photogrammetry in physical geography. *Prog. Phys. Geogr.* **2016**, *40*, 247–275. [CrossRef]
23. Harwin, S.; Lucieer, A.; Osborn, J. The impact of the calibration method on the accuracy of point clouds derived using unmanned aerial vehicle multi-view stereopsis. *Remote Sens.* **2015**, *7*, 11933–11953. [CrossRef]
24. Gómez-Gutiérrez, Á.; de Sanjosé-Blascom, J.J.; Lozano-Parra, J.; Berenguer-Sempere, F.; de Matías-Bejarano, J. Does HDR pre-processing improve the accuracy of 3D models obtained by means of two conventional SfM-MVS software packages? The case of the Corral del Veleta rock glacier. *Remote Sens.* **2015**, *7*, 10269–19294. [CrossRef]
25. Sissons, J.B. The Loch Lomond Advance in the Lake District, northern England. *Trans. R. Soc. Edinb. Earth Sci.* **2015**, *71*, 13–27. [CrossRef]
26. McDougall, D.A. The geomorphological impact of Loch Lomond (Younger Dryas) Stadial plateau icefields in the central Lake District, northwest England. *J. Quat. Sci.* **2001**, *16*, 531–543. [CrossRef]
27. Graham, D.J.; Hambrey, M.J. Sediments and landforms in an upland glaciated-valley landsystem, upper Ennerdale, English Lake District. In *Glacial Sedimentary Processes and Products*; Hambrey, M.J., Christoffersen, P., Glasser, N.F., Hubbard, B., Eds.; International Association of Sedimentologists: Oxford, UK, 2007; pp. 235–256.
28. Immerzeel, W.W.; Kraaijenbrink, P.D.A.; Shea, J.M.; Shrestha, A.B.; Pellicciotti, F.; Bierkens, M.F.P.; de Jong, S.M. High-resolution monitoring of Himalayan glacier dynamics using unmanned aerial vehicles. *Remote Sens. Environ.* **2015**, *150*, 93–103. [CrossRef]
29. Carrivick, J.L.; Smith, M.W.; Quincey, D.J. *Structure from Motion in the Geosciences*; Wiley-Blackwell: Oxford, UK, 2016; p. 208.
30. James, M.R.; Robson, S. Mitigating systematic error in topographic models derived from UAV and ground-based image networks. *Earth Surf. Process. Landf.* **2014**, *39*, 1413–1420. [CrossRef]